Catalysis Today 213 (2013) 58–64

Contents lists available at SciVerse ScienceDirect

Catalysis Today

journal homepage: www.elsevier.com/locate/cattod

Pt catalyst supported on α-Al_2O_3 modified with CeO_2 and ZrO_2 for aqueous-phase-reforming of glycerol

Maria L. Barbelli[a,b], Francisco Pompeo[a,b], Gerardo F. Santori[a,b], Nora N. Nichio[a,b,*]

[a] Facultad de Ingeniería, PIDCAT, Universidad Nacional de La Plata, 1 esq 47, 1900 La Plata, Argentina
[b] CINDECA, Facultad de Ciencias Exactas, Universidad Nacional de La Plata, CCT La Plata- CONICET, 47 N° 257, 1900 La Plata, Argentina

ARTICLE INFO

Article history:
Received 3 December 2012
Received in revised form 5 February 2013
Accepted 11 February 2013
Available online 10 May 2013

Keywords:
Hydrogen
APR
Biomass
Glycerol
Platinum

ABSTRACT

The catalytic conversion of renewable sources using processes with low energy consumption is expected to reduce damage on the environment. In this sense, significant progress in reforming of alcohol from biomass has been made.

The aim of the present work was to study the aqueous phase reforming (APR) of glycerol using Pt catalysts supported on SiO_2, α-Al_2O_3, and α-Al_2O_3 modified with CeO_2 and ZrO_2 ($Ce_4Zr_1\alpha$).

The higher activity and H_2 selectivity would be related to the less particle size or higher metal dispersion of catalysts. The redox properties of the support $Ce_4Zr_1\alpha$ favor the water gas shift reaction, increasing the yield H_2. The Pt/$Ce_4Zr_1\alpha$ shows deactivation by a fast sintering, however this catalyst presents the best performance; even after three reaction cycles and regeneration.

1. Introduction

In recent years, the benefits of generating hydrogen from renewable sources and by means of processes with low energetic requirements have been investigated. In this context, oxygenated hydrocarbons coming from the biomass constitute a promissory source for sustainable hydrogen production.

Nowadays, alcohols, as methanol, ethanol and polyols as ethylene glycol, glycerol and sorbitol are found among most studied organic molecules to obtain hydrogen by steam reforming and aqueous phase reforming (APR) [1–4].

The APR has several advantages over steam reforming, for example lower energy consumption, since it avoids the vaporization of water and alcohol. Additionally, the lower APR temperature minimizes undesirable decomposition reactions and favors the water–gas shift reaction (WGS).

Catalytic systems based on metals of group VIII are cited in bibliography for APR of oxygenated hydrocarbons [2–8]. Wen et al. using a fixed-bed flow reactor have reported for APR of glycerol the decreasing order in the yield to H_2: Pt > Cu > Ni > Co [9]. The activity, stability and composition of gas products were significantly affected by the nature of the metal component, acidity and basicity, and hydrothermal stability of the support. Basic support resulted in high activity and higher hydrogen molar concentration, whereas acidic support and neutral support increase alkane formation. With respect to the study of different supports, APR of ethylene glycol was studied over Pt supported on TiO_2, Al_2O_3, carbon, SiO_2, SiO_2–Al_2O_3, ZrO_2, CeO_2 and ZnO as well as Pt-black [10]. Based on the turnover frequency for H_2, Pt black, Pt supported on Al_2O_3, TiO_2 and carbon exhibited the highest activity. Pt supported on Al_2O_3, and to a lesser extent ZrO_2, exhibits high selectivity for production of H_2 and CO_2. In contrast, Pt supported on carbon, TiO_2, SiO_2–Al_2O_3 and Pt-black produce measurable amounts of liquid–phase compounds that would lead to alkanes at higher conversions (e.g., ethanol, acetic acid, acetaldehyde) [10].

Manfro et al. studied Ni/CeO_2 in APR of glycerol at 250–270 °C [11]. These CeO_2-supported catalysts showed lower formation of methane than alumina supported nickel.

Menezes et al. studied Pt catalysts supported on Al_2O_3, ZrO_2, MgO and CeO_2 in APR of glycerol [12]. All catalysts led to a hydrogen-rich gas phase. However, a good potential activity with high production of hydrogen and low concentration of undesired hydrocarbons was accomplished over the catalysts supported on MgO and ZrO_2.

Iriondo et al. studied the APR of glycerol using a fixed-bed flow reactor with Ni and Pt monometallic and bimetallic catalysts supported on γ-Al_2O_3 and La_2O_3-modified γ-Al_2O_3. PtNi catalysts were the most active, whereas Ni catalysts experienced increasing deactivation as the temperature increased. The presence of La_2O_3 improved this catalytic behavior toward lighter gaseous products [13].

Wawrzetz et al. indicated that the initial reaction steps are dehydrogenation and dehydration. The dehydrogenation of hydroxyl groups at primary carbon atoms is followed by decarbonylation and

* Corresponding author. Tel.: +54 2214210711.
E-mail address: nnichio@quimica.unlp.edu.ar (N.N. Nichio).

0920-5861/$ – see front matter © 2013 Elsevier B.V. All rights reserved.
http://dx.doi.org/10.1016/j.cattod.2013.02.023

subsequent water gas shift or by disproportionation to the alcohol followed by decarboxylation. Larger Pt particles favor hydrodeoxygenation over complete deconstruction to hydrogen and CO_2 [14].

The present contribution has as an aim to analyze the effect of the particle size and the role of the supports on the activity and selectivity to gaseous and liquid products in the APR of glycerol. To analysis the particle size effect, Pt/SiO_2 samples were prepared through different methods (impregnation and ionic exchange), obtaining different particle sizes on a support with neutral characteristics. To study the effect of the support, SiO_2, α-Al_2O_3 and α-Al_2O_3 modified with Ce and Zr were used. Finally, we studied with particular emphasis the stability of the catalyst which results more active and selective. The post-reaction samples were characterized by XPS, TEM and Raman, in order to determine the mechanism responsible for the deactivation.

2. Experimental

2.1. Catalyst preparation

The Pt catalysts (~1 and 2 wt%) supported on SiO_2 (Aerosil 200, Degussa) were prepared at room temperature using two methods: ionic exchange (ie) and incipient wetness impregnation (iwi), in order to obtain catalysts with different metallic dispersion.

For the preparation by ionic exchange (cationic), the silica was suspended in NH_4OH.aq/under stirring prior to the addition of the $[Pt(NH_3)_4]Cl_2$ solution, having a concentration so as to obtain 1 and 2 wt% Pt exchanged on the silica. The solid was kept under stirring for 24 h at 25 °C, in order to be able to obtain a uniform distribution of platinum over the silica surface, as was indicated by Goguet et al. [15]. Subsequently, the suspension was separated by filtration under vacuum. The solid was repeatedly washed, dried at 105 °C, calcined in air at 500 °C, leading to the "$1PtSi_{(ie)}$" and "$2PtSi_{(ie)}$" catalysts.

The sample $2PtSi_{(Sintered)}$ was generated by sintering the $2PtSi_{(ie)}$ catalyst at 800 °C with H_2 flow saturated with steam. The sample $2PtSi_{(iwi)}$ was prepared by impregnation with $[Pt(NH_3)_4]Cl_2$ in aqueous solution.

The Pt catalysts (1 wt%) supported on α-Al_2O_3 and α-Al_2O_3 modified with CeO_2 and ZrO_2 were prepared at room temperature by impregnation (iwi) with a H_2PtCl_6. Commercial α-Al_2O_3 Rhone Poulenc (Spheralite 512; surface area around 10 $m^2\,g^{-1}$) was used as base support. Modified supports were prepared by impregnations of α-Al_2O_3 with $ZrO(NO_3)_2{\cdot}xH_2O$ (Aldrich) and $Ce(NO_3)_3{\cdot}6H_2O$ (Alpha) aqueous solutions, with 4 wt% CeO_2 and 1 wt% ZrO_2 (denoted as $Ce_4Zr_1\alpha$). The solids were dried at 105 °C and calcined in air at 500 °C.

2.2. Catalyst characterization

The Pt content was determined by atomic absorption spectrometry (AAS). The calibration curve method was used, with standards prepared in the laboratory. The equipment utilized was an IL Model 457 spectrophotometer, with single channel and double beam. The light sources were hollow monocathode lamps.

Mean particle size was determined by TEM and obtained in a TEM JEOL 100 C instrument. A graphite pattern was used for calibration. To estimate the average particle size, the particles were considered spherical and the diameter volume-area was calculated by using the following expression

$$d_{va} = \frac{\sum ni \cdot di^3}{\sum ni \cdot di^2} \quad (1)$$

where ni is the number of particles with diameter di.

Hydrogen chemisorption measurements were carried out in dynamic equipment with a TCD detector. Samples were reduced in H_2 at 500 °C for 1 h, cooled in H_2 up to 400 °C, flushed with Ar for 2 h at 400 °C and then cooled up to room temperature in Ar flow. Hydrogen pulses were then injected up to saturation. Dispersions were estimated from the hydrogen amount consumed, assuming an adsorption stoichiometry H/Pt = 1.

Temperature programmed reduction tests (TPR) were performed using a conventional dynamic equipment and the response was measured using a thermal conductivity detector. The feed flow was H_2/N_2 ratio of 1/9 and the heating rate was 10° min^{-1} from room temperature up to 1000 °C.

The XPS analysis was carried out in a multi-technique system (Specs), equipped with a dual Mg/Al X-ray source and a hemispherical PHOIBOS 150 analyzer operating in the fixed analyzer transmission (FAT) mode. The spectra were obtained with a pass energy of 30 eV and an Al-Kα anode operated at 200 W. The pressure during the measurement was less than 2×10^{-8} mbar. The samples were subjected to a reduction during 10 min at 500 °C in H_2 5%/Ar flux in the pretreatment chamber of the equipment.

The Raman spectra were recorded with a TRS-600-SZ-P Jasco Laser Raman instrument, equipped with a CCD (charge coupled device) with the detector cooled with liquid N_2. The excitation source was the 514.5 nm line of a Spectra 9000 Photometrics Ar ion laser. The laser power was set at 30 mW. The spectral resolution was 4 cm^{-1}.

2.3. Catalytic tests

The APR experiments were carried out in a High Pressure Reactor BR-100 system, from Berghof Instruments, with a volume of 100 mL, operated in batch mode. The magnetic stirring was set at 900 rpm. The reactive mixture, 12 cm^3, was an aqueous solution of 10 wt% alcohol and the catalyst concentration was 4.2 wt%. As considered thermodynamically elsewhere [16], the conversion of glycerol to hydrogen and carbon dioxide is highly favorable at relatively low temperature (~227 °C), for this reason the reaction was studied in the range 200–250 °C.

In a typical experiment, the catalyst was reduced ex situ at 500 °C for 1 h in H_2 flow (30 $cm^3\,min^{-1}$) using a heating rate of 10 °C min^{-1}. Then, the catalyst was introduced in the reaction media under H_2 flow at room temperature. Subsequently, the reactor was purged with N_2 (Air Liquide, 99.99%) and heated to reaction temperature. The catalytic tests were performed at 200, 225 and 250 °C, resulting in autogenous pressure of 16, 24 and 44 bar respectively.

The main reactions involved in the APR are represented in Eqs. (2)–(4)

$$C_3H_8O_3 \leftrightarrow 3CO + 4H_2 (\text{GLY decomposition}) \quad (2)$$

$$CO + H_2O \leftrightarrow CO_2 + H_2 (\text{Water–gas shift reaction}) \quad (3)$$

$$C_3H_8O_3 + 3H_2O \leftrightarrow 3CO_2 + 7H_2 (\text{Reforming reaction}) \quad (4)$$

The catalytic activity is expressed as the conversion to gaseous products (X^G) and the total conversion (X^T), defined as:

$$X_i^G = \frac{N_{CO} + N_{CO_2} + N_{CH_4}}{n \times N_i^o} \times 100 \quad (5)$$

where

N_i^o, initial moles of alcohol;
N_{CO}, N_{CO_2} and N_{CH_4}, moles of CO, CO_2 and CH_4 in gas products;
n, 3 (number of carbon atoms in the alcohol molecule)

Table 1
Characterization of the studied catalysts. BET surface areas, metal content by atomic absorption, mean particle size (d_{av}) by TEM, H_2 chemisorption (H/Pt ratio) and TPR results.

Catalyst	S_{BET} support ($m^2\ g^{-1}$)	Pt (wt%)	d_{av} (nm)	Dispersion (H/Pt)	TPR peaks (°C)	
		AA			LT[a]	HT[b]
$2PtSi_{(iwi)}$	200	2.3	5.5	0.20	147	400
$2PtSi_{(ie)}$	200	2.0	2.2	0.60	155	410
$2PtSi_{(Sintered)}$	200	2.0	6.2	0.20	130	400
$PtSi_{(ie)}$	200	0.9	2.4	0.60	110	410
Ptα	10	1.0	2.5	0.53	107	427
$PtCe_4Zr_1\alpha$	8	1.1	2.1	0.60	134	391

[a] LT, low temperature.
[b] HT, high temperature.

$$X_i^T = \frac{N_i^o - N_i^f}{N_i^o} \times 100 \quad (6)$$

where

N_i^f, final moles of alcohol

The selectivity to carbon products (SC_n%), Yield H_2% and H_2 Selectivity % were defined as:

$$SC_n\% = \frac{(\text{mol of the product}) \times (\text{number of carbon atoms in the product})}{\text{mol of glycerol consumed} \times 3} \times 100 \quad (7)$$

$$\text{Yield } H_2\% = \frac{\text{mol of } H_2}{\text{mol of glycerol charged} \times 7} \times 100 \quad (8)$$

$$H_2 \text{ Selectivity}\% = \frac{\text{molecules of } H_2 \text{ produced}}{\text{C atoms in gas products}} \times \frac{1}{R} \times 100 \quad (9)$$

where R is the H_2/CO_2 reforming ratio of 7/3 for glycerol.

2.4. Analysis of products

The analysis of gaseous products was performed with a gas chromatograph Shimadzu GC-8A equipped with a column of 10 m and 1/8″ HayeSep DB 110-120 and GC/TCD detector. The liquid products were analyzed by gas chromatography with GC/FID and mass spectrometry CG/MS detector (Shimadzu GCMS-QP5050A) with 50 m (0.2 mm and 0.5 μm) HP-PONA capillary column. The accuracy of the measured values was within 5% and the experiments could be reproduced with a relative error of 10%.

3. Results and discussion

3.1. Catalyst characterization

Table 1 presents supports used, showing that S_{BET} values are from 8 $m^2\ g^{-1}$ for $Ce_4Zr_1\alpha$ to 200 $m^2\ g^{-1}$ for SiO_2. In a previous work we have reported the superficial acidity through an indirect method by catalytic decomposition reaction of isopropanol (IPA). Thus, the acidity of supports does not differ significantly but decreases in the order of α-Al_2O_3 > $Ce_4Zr_1\alpha$ > SiO_2. Moreover, we have demonstrated that the best support properties are achieved with Ce:Zr ratio 4:1, and the $Ce_4Zr_1\alpha$ support consists of patches of mixed oxide of $Ce_{0.8}Zr_{0.2}O_2$ over α-Al_2O_3 [17].

Physicochemical properties of Pt catalysts are indicated in Table 1. The particle size distribution determined from TEM micrographs by at least calculating 100 particles was very narrow with a mean particle size (d_{TEM}) of about 2–6 nm.

The impregnated catalyst $2PtSi_{(iwi)}$ showed less metallic dispersion and bigger particle size than that prepared through ionic exchange ($2PtSi_{(ie)}$). The treatment of $2PtSi_{(ie)}$ at 800 °C in H_2 flow saturated with steam resulted in the sintering of Pt particles to a d_{TEM} = 6.2 nm (sample $2PtSi_{(Sintered)}$). The Pt content increase from ~1 to 2 wt% does not affect properties of $PtSi_{(ie)}$ catalysts as it was observed in Table 1. It can also be observed that $PtCe_4Zr_1\alpha$ presents slightly greater dispersions value than Ptα. This fact would be indicating a higher interaction between the metallic precursor and the modified support, compared with α-Al_2O_3.

Reduction profiles obtained by TPR show the presence of two peaks, the first one around 107–155 °C and the second between 390 and 430 °C (denoted as LT and HT respectively in Table 1). According to the literature, the lowest temperature peak can be assigned to the reduction of Pt oxide species weakly interacting with support [18,19]. With respect to the high temperature peak, Ho et al. reported for Pt/SiO_2 catalysts, that the species with more interaction $Pt–(O–Si\equiv)_y^{n-y}$ (n = +2 or +4) are reduced to temperatures over 400 °C [18]. Moreover, several authors reported for Pt/Al_2O_3 catalysts, that the less important second reduction band is assigned to the reduction of Pt oxychlorinated species (PtO_xCl_y) in strong interaction with the support [19–21].

Fig. 1 shows programmed temperature reduction profiles for $PtSi_{(ie)}$, Ptα and $PtCe_4Zr_1\alpha$. For $PtSi_{(ie)}$ sample, the principal contribution is the peak at T > 350 °C, evidencing the major interaction Pt-support. For $PtCe_4Zr_1\alpha$ there is a low-temperature hydrogen consumption (LT) that is higher to the complete reduction of the Pt, which would indicate that, as it has been cited in the references, Pt favors the reduction of Ce [22,23].

Table 2
APR results of glycerol (GLY), ethylene glycol (EG), propylene glycol (PG) and acetol (AC) with the $2PtSi_{(ie)}$ catalyst. Reaction condition: P = 24 bar, T: 225 °C, reaction time: 2 h.

%	APR			
	GLY	EG	AC	PG
X^G	9	11	13	10
X^T	15	13	72	21
SCO	0.1	0.7	0.1	0.5
SCH_4	3.8	7.2	9.0	12.0
SCO_2	58.0	80.0	17.0	34.0
Liquid products				
$SC_1 + SC_2$	17.1	12.1	6.9	18.5
SC_3	21.0	–	67.0	35.0

3.2. Catalytic tests

APR results of glycerol (GLY) at 225 and 250 °C using SiO_2, α-Al_2O_3, and $Ce_4Zr_1\alpha$ (without Pt) showed negligible levels of conversion (X^T around 1%).

In Table 2 the results of the APR of GLY at 225 °C with the catalyst $2PtSi_{(ie)}$ are shown. The gaseous products were mainly H_2, CO_2 and CH_4, being the selectivity to CO_2 (SCO_2) representative of the selectivity to the reforming reaction (reaction (4)). The low CO content near to 1000 ppm in gaseous products would be indicating that the CO can be quickly converted to CO_2 through the WGS reaction (reaction (3)). In Table 2 it is also indicated the selectivity to liquid products grouped by the number of carbon atoms: SC_1 (methanol), SC_2 (ethanol and ethylene glycol) and SC_3 (acetone, 1-propanol, acetol, propylene glycol). Of these liquid products, the main compound was propylene glycol (~50% molar in the liquid).

APR tests of ethylene glycol (EG), acetol (AC) and propylene glycol (PG) allowed for the evaluation of their reactivity to the cleavage of C—C bond vs. cleavage of C—O bond, with the aim of identifying the main intermediaries of the reforming reaction and the lateral products. While methanol, ethanol and 1-propanol were very stable alcohols and not very reactive at 225 °C, the acetol, ethylene glycol and propylene glycol showed remarkable differences in their reactivity. The APR of EG showed the highest selectivity to cleavage

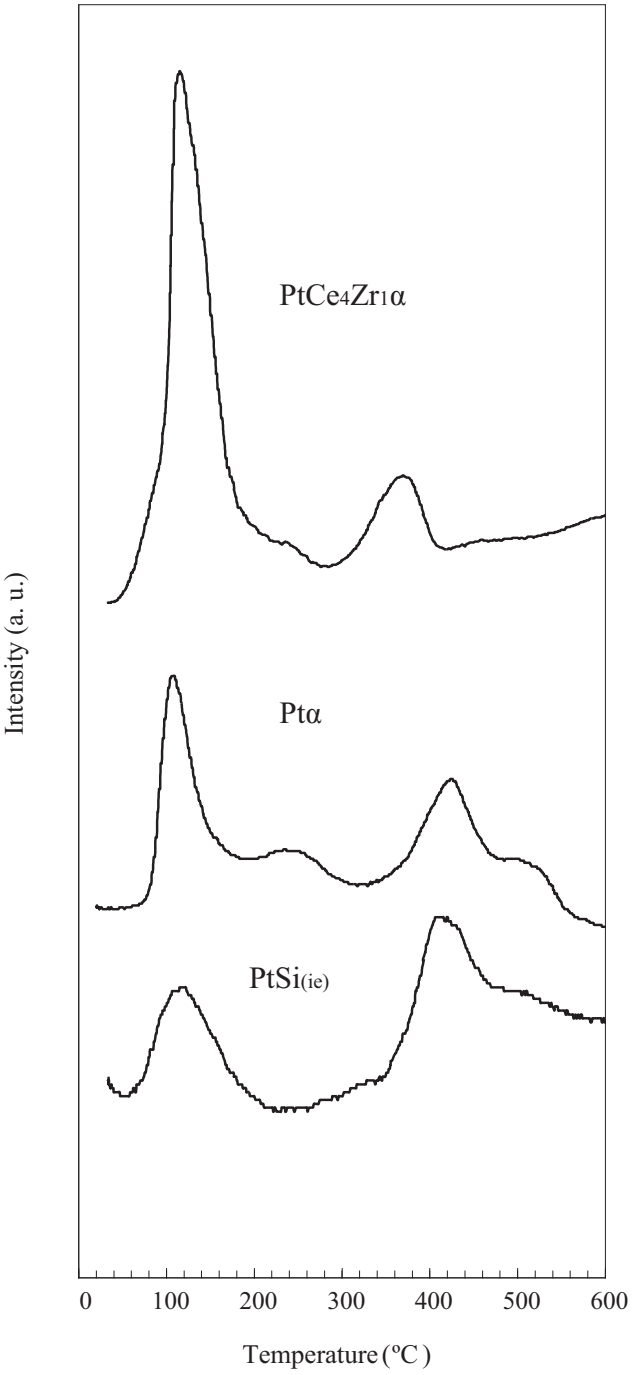

Fig. 1. Temperature programmed reduction (TPR) profiles for $PtSi_{(ie)}$, $PtCe_4Zr_1\alpha$ and Ptα catalysts.

of C—C bond reactions and therefore higher selectivity to the reforming (SCO_2 = 80%, Table 2). On the other hand, the APR of the AC showed the lowest selectivity to cleavage of C—C bond reactions (SCO_2 = 17%, Table 2). The APR of the PG showed a higher selectivity to reforming than the AC but lower than GLY.

These results would indicate that the EG is a reforming reaction intermediary, while the AC is a lateral product derived from the cleavage of C—O bond reactions. The high content of PG in the liquid products of the APR of GLY could be explained by the hydrogenation of the AC.

3.2.1. Metallic dispersion effect

From Table 1, it is possible to observe that the catalysts supported on SiO_2 denoted as $2PtSi_{(iwi)}$, $2PtSi_{(ie)}$, and $2PtSi_{(Sintered)}$, show different metallic dispersions over a neutral support. In Table 3 the conversion and selectivity to gaseous and liquid products are shown. As was previously indicated, the selectivity SC_3 groups the lateral products: propylene glycol, acetol and to a lesser extent acetone and 1-propanol. The $2PtSi_{(ie)}$ catalyst showed the best selectivity and yield to H_2 (SH_2 = 81%, Yield H_2 = 8%). It can be observed that the smallest particle size of the catalyst $2PtSi_{(ie)}$ would favor the cleavage of C—C bond (SCO_2 = 58%), against the cleavage of C—O bond and hydrogenations (SC_3 = 21%), which are very important for the H_2 production.

Table 3
Results of APR of GLY with 2PtSi catalyst. Reaction condition: P = 24 bar, T: 225 °C, reaction time: 2 h.

%	$2PtSi_{(iwi)}$	$2PtSi_{(ie)}$	$2PtSi_{(Sintered)}$
Dispersion	20	60	20
X^G	5	9	4
X^T	17	15	16
SH_2	68	81	75
SCO	0.01	0.10	0.14
SCH_4	0.6	3.8	0.4
SCO_2	29.0	58.0	28.0
H_2/CO_2	1.7	2.0	1.9
Yield H_2	4.0	8.0	3.0
Liquid products			
SC_1	2.5	2.3	3.3
SC_2	18.4	14.8	18.2
SC_3	49.5	21.0	50.0

Claus et al. postulate that the selectivity to H_2 increase with increasing Pt particle size because of the enhanced rate of cleavage C–C bond on Pt ensembles on low index metal surfaces [24]. However, Lercher et al. have reported that the higher relative concentration of edges and kinks on the surface of small Pt particles favors the cleavage of C—H bond and C—C bonds [14]. The catalysts $2PtSi_{(iwi)}$ and $2PtSi_{(Sintered)}$ have a similar mean particle size (~5.5–6.2 nm), and the results of the activity show that the biggest particle size with respect to $2PtSi_{(ie)}$ (2.2 nm) favors the cleavage of C—O bond and hydrogenations (SC_3 ~ 50%). Our results are in agreement with what was postulated by Lercher et al.

3.2.2. Effect of the support

In order to analyze the effect of the support, catalysts with similar metallic content (~1 wt%) and similar metallic dispersion (~0.6) were selected: $PtSi_{(ie)}$, Ptα and $PtCe_4Zr_1\alpha$. Table 4 shows the results of the APR of GLY. Comparing the results obtained at 250 °C, shown in Table 4, it was observed that $PtCe_4Zr_1\alpha$ turned out to be the most active (X^G = 29%), with the highest selectivity to reforming (SCO_2 = 45%), lowest selectivity to lateral products (SC_3 = 35%) and highest yield to H_2 (Yield H_2 = 20%). This could be associated with the redox properties of the support $Ce_4Zr_1\alpha$. While in PtSi

Table 4
Results of APR of GLY. Reaction condition: P = 44 bar, T: 250 °C, reaction time: 2 h.

%	$PtSi_{(ie)}$	Ptα	$PtCe_4Zr_1\alpha$
Dispersion	60	53	60
X^G	12	18	29
X^T	29	43	60
SH_2	78	71	81
SCO	0.1	0.1	0.01
SCH_4	4.0	1.4	2.0
SCO_2	37.0	40.0	45.0
H_2/CO_2	2.0	1.7	1.7
Yield H_2	9	13	20
Liquid products			
SC_1	1.0	1.0	1.3
SC_2	11.6	12.9	16.5
SC_3	46.0	44.6	35.3

Table 5
Results of APR of GLY with $PtCe_4Zr_1\alpha$ catalyst. Reaction condition: P = 44 bar, T: 250 °C, reaction time: 2 h.

%	Tests			
	1°	2°	3°	4°
X^G	29	24	23	31
X^T	60	68	80	69
SCO_2	45	35	27	40
SC_3	35	42	47	40
Yield H_2	20	18	17	17

Tests Nos. 1, 2 and 3: three successive reactions, the catalyst was reused after being washed with water in situ.
Test No. 4: test was done with the sample used in test No. 3, regenerated in air flow at 500 °C.

and Ptα water activation is only produced over the metallic site, in $PtCe_4Zr_1\alpha$ the mixed oxide of $Ce_{0.8}Zr_{0.2}O_2$ would participate.

It has been indicated in the bibliography that Pt supported on reducible carriers such as TiO_2 and ZrO_2 generally showed higher activity for the WGS reaction [25]. As regards supports with Ce and Zr, it has been proposed for WGS reaction a mechanism via formate. In this mechanism, the formation of bridging OH groups occur at Ce^{3+} defect sites and the presence of Zr^{+4}, in the interaction with Ce^{+3}, facilitates the decomposition of the formate [26].

3.2.3. Catalytic stability of $PtCe_4Zr_1\alpha$

The stability of $PtCe_4Zr_1\alpha$ was studied due since it resulted the most active and selective catalyst to the reforming reaction of glycerol. The results of three reaction tests are shown in Table 5, where the catalyst was reused after being washed with water in situ. The fourth reaction test was done with the sample used in test No. 3, regenerated in air flow at 500 °C during 1 h and reduced to the same temperature.

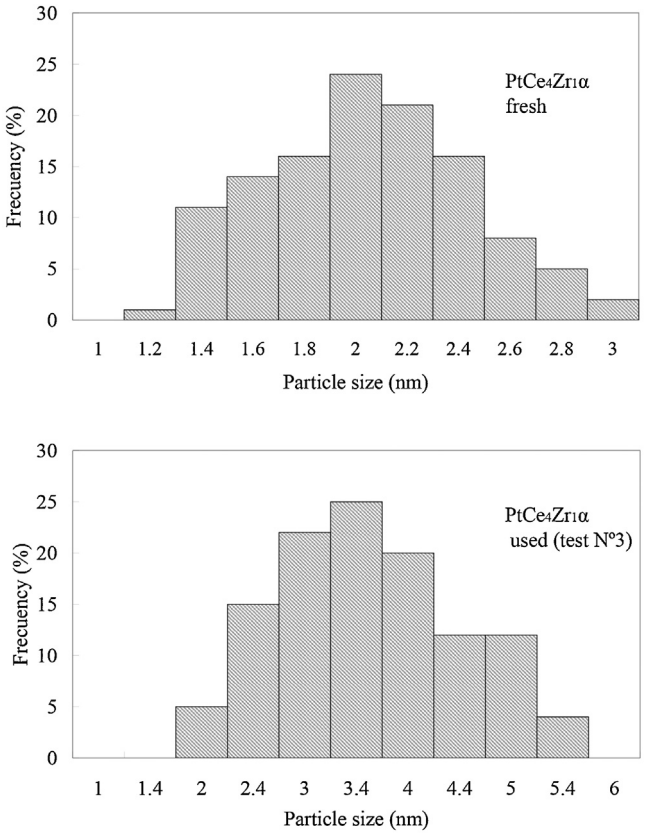

Fig. 2. Particle size distribution determined by TEM.

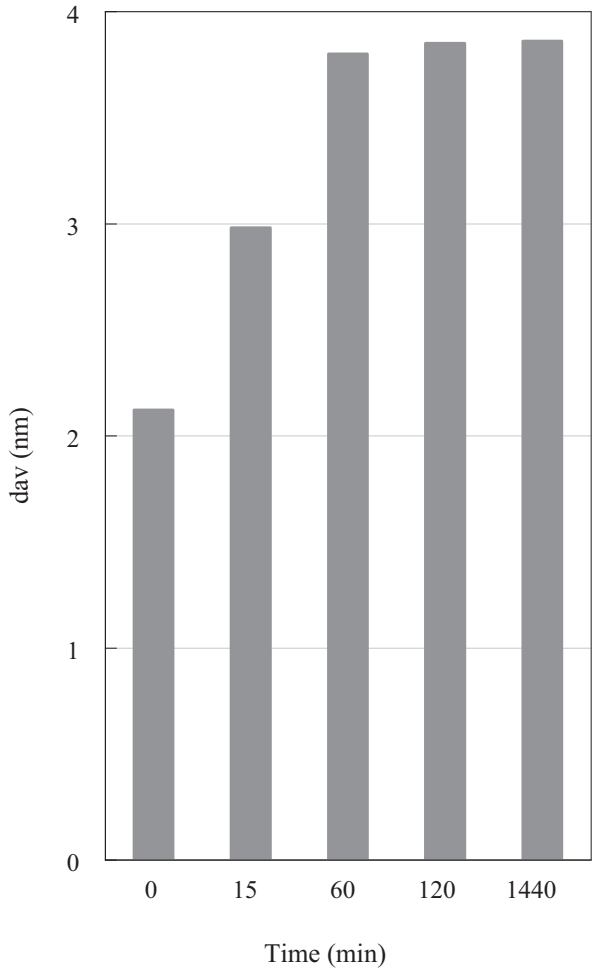

Fig. 3. Change in dispersion as a function of reaction time as measured by TEM for $PtCe_4Zr_1\alpha$. Each point corresponds to a different batch test.

It is observed that after the 1st reaction test, the catalyst shows some deactivation. In tests No. 2 and 3, the conversion to gaseous products and the SCO_2 selectivity decrease, while the selectivity to lateral products SC_3 increase, leading to a yield loss to H_2. After the regeneration, test No. 4, it is observed that the conversion to gases is recovered, but not the yield to H_2 due to the conversion to lateral liquid products (Table 5).

The characterization of the fresh and used samples by TEM, Raman and XPS permitted the analysis of the possible causes of the observed deactivation.

The increase in the particle size with the reaction time was determined by TEM (Fig. 2). It was observed that in $PtCe_4Zr_1\alpha$ a fast sintering is produced at 15 min, which later remains stable (Fig. 3). These results allowed confirming the severe hydrothermal conditions that the APR process represents.

By Raman it was observed that the spectrum of the post-reaction sample "3" did not show presence of any carbonaceous deposits of the coke in the range 1200 and 1700 cm^{-1}, but a high band was observed at 4400 cm^{-1} which could be attributed to molecules containing groups –CH, aromatic aldehyde groups and/or cyclopropane groups (Fig. 4). This would indicate that besides the sintering there is a contribution due to the chemisorption of the reaction intermediate species. Due to the fact that in the Raman spectrum of the regenerated catalyst the band at 4400 cm^{-1} disappears, the thermal treatment with air flow at 500 °C allowed the elimination of these chemisorbed compounds.

Table 6
Characterization by XPS. Binding energies (eV) and surface atomic fraction for $PtCe_4Zr_1\alpha$ catalysts.

	Pt $4f_{7/2}$ (eV)	Ce $3d_{5/2}$ (eV)	Zr $3d_{5/2}$ (eV)	Al 2p (eV)	(Pt/Al)	(Pt/Zr)	(Pt/Ce)
$PtCe_4Zr_1\alpha$ fresh	70.7	881.2 (v) 884.8 (v′) 915.9 (u‴, 4.6%)	181.6	73.8	0.030	2.03	3.5
$PtCe_4Zr_1\alpha$ regenerated	70.7	881.6 (v) 885.2 (v′) 916.8 (u‴, 3%)	181.8	74.2	0.014	1.18	2.89

In Table 6 the results obtained by XPS for the catalyst $PtCe_4Zr_1\alpha$ fresh and regenerated are shown, where the binding energy (BE) of the Pt $4f_{7/2}$, Ce $3d_{5/2}$, Zr $3d_{5/2}$ and Al 2p is shown. The occurrence of a strong interaction between ceria and zirconia in $PtCe_4Zr_1\alpha$ is evidenced by the decrease in the BE of Zr $3d_{5/2}$ (181.6–181.8 eV) with respect to the value for ZrO_2 (182.5 eV), as reported in the bibliography [27]. For the fresh and used sample it is observed in the region corresponding to $Pt4f_{7/2}$ at 70.7 eV, there appears only one peak indicating the complete reduction of platinum.

The Ce 3d region shows presence of both Ce^{4+} and Ce^{3+} oxidation states. For Ce^{4+} the Ce $3d_{5/2}$ and Ce $3d_{3/2}$ lines (separated by about 18.5 eV) are characterized by three contributions denoted as v, v″, v‴ and u, u″, u‴, respectively [28]. Because the u‴ peak arises exclusively from Ce^{4+}, it can be used as quantitative measure of Ce^{4+} amount and by difference quantify the Ce^{3+}. As it has been indicated in the bibliography, if all the Ce is found as Ce^{+4}, the integrated area of the u‴ component with respect to the total Ce 3d area should constitute around 14% of total integral intensity [29]. The results of the catalysts (fresh and regenerated), in Table 6, show that the presence of Pt^0, Ce^{+3} and Zr^{+4} is confirmed, which allows to explain the role of the support in the WGS reaction.

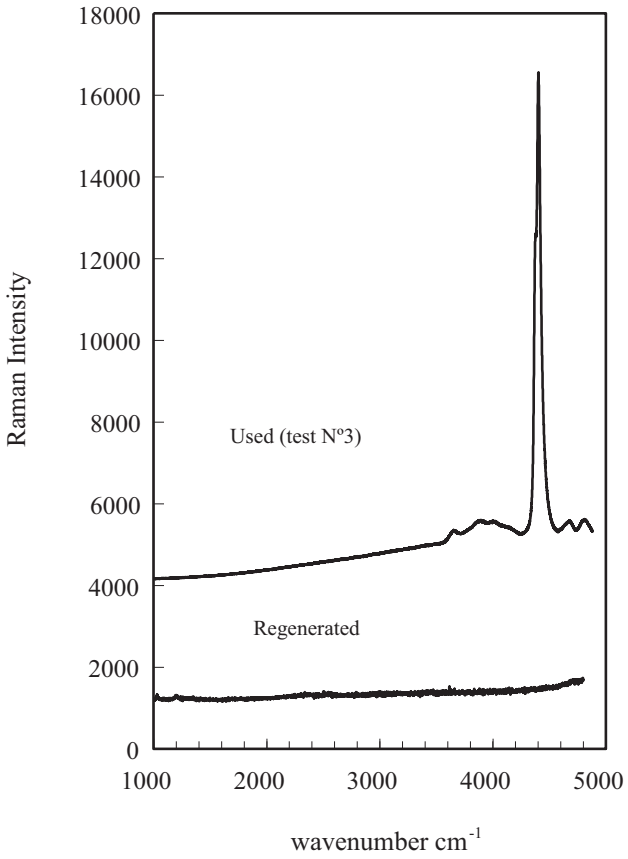

Fig. 4. Raman spectra of $PtCe_4Zr_1\alpha$ catalyst used in Test 3 and regenerated.

Furthermore, it is observed that the intensity relations of the Pt to the elements of the support (Al, Zr and Ce) decrease in the regenerated sample, which would be confirming the loss of the platinum superficial by sintering.

The $PtCe_4Zr_1\alpha$ systems presents the best performance of the catalysts studied here, due to the fact that even after three reaction cycles and the regeneration, it presents higher activity and selectivity compared to the fresh Ptα and PtSi catalysts.

4. Conclusions

In this work, we studied Pt catalysts supported on SiO_2, α-Al_2O_3, and α-Al_2O_3 modified with CeO_2 and ZrO_2 in the aqueous phase reforming (APR) of glycerol. It can be observed that the smallest particle size would favor the cleavage of C—C bond, against the cleavage of C—O bond and hydrogenations reactions, which are very important for the reforming. The $PtCe_4Zr_1\alpha$ turned out to be the most active (X^G = 29%), with the highest selectivity to reforming (SCO_2 = 45%) and highest yield to H_2 (Yield H_2 = 20%). The presence of Pt^0, Ce^{+3} and Zr^{+4} is confirmed by XPS, which allows explaining the role of the support in the WGS reaction.

The characterization of the fresh and used samples by TEM, Raman and XPS allowed determining that the principal cause of the observed deactivation is a fast sintering which later remains stable. The $PtCe_4Zr_1\alpha$ system presents the best performance; even after three reaction cycles and the regeneration, it presents more activity and selectivity compared to the Ptα and PtSi fresh catalysts.

Acknowledgements

We thank the financial support from ANPCyT PICT No 1962, Project I175 UNLP and CONICET PIP 542. M.L.B. thanks the fellowship received from PRH 200-7. Laura Cornaglia for the XPS measurements is gratefully acknowledged.

References

[1] V. Mas, M.L. Bergamini, G. Baronetti, N. Amadeo, M. Laborde, Topics in Catalysis 51 (2008) 39–48.
[2] R.R. Soares, D.A. Simonetti, J.A. Dumesic, Angewandte Chemie International Edition 45 (2006) 3982–3985.
[3] M.B. Valenzuela, C.W. Jones, P.K. Agrawal, Energy and Fuels 20 (2006) 1744–1752.
[4] E. Gürbüz, E. Kunkes, J.A. Dumesic, Applied Catalysis B: Environmental 94 (2010) 134–141.
[5] D.L. King, L. Zhang, G. Xia, A.M. Karim, D.J. Heldebrant, X. Wang, T. Peterson, Y. Wang, Applied Catalysis B: Environmental 99 (2010) 206–213.
[6] G.W. Huber, J.W. Shabaker, S.T. Evans, J.A. Dumesic, Applied Catalysis B: Environmental 62 (2006) 226–235.
[7] J.W. Shabaker, R.R. Davda, G.W. Huber, D. Cortright, J.A. Dumesic, Journal of Catalysis 215 (2003) 344–352.
[8] R.R. Davda, J.W. Shabaker, G.W. Huber, D. Cortright, J.A. Dumesic, Applied Catalysis B: Environmental 56 (2005) 171–186.
[9] G. Wen, Y. Xu, H. Ma, Z. Xu, Z. Tian, International Journal of Hydrogen Energy 33 (2008) 6657–6666.
[10] J.W. Shabaker, G.W. Huber, R.R. Davda, D. Cortright, J.A. Dumesic, Catalysis Letters 88 (2003) 1–8.
[11] R.L. Manfro, A.F. da Costa, N.F.P. Ribeiro, M.V.M. Souza, Fuel Processing Technology 92 (2011) 330–335.
[12] A.O. Menezes, M.T. Rodrigues, A. Zimmaro, L.E.P. Borges, M.A. Fraga, Renewable Energy 36 (2011) 595–599.

[13] A. Iriondo, J.F. Cambra, V.L. Barrio, M.B. Guemez, P.L. Arias, M.C. Sanchez-Sanchez, R.M. Navarro, J.L.G. Fierro, Applied Catalysis B: Environmental 106 (2011) 83–93.
[14] B. Wawrzetz, A. Peng, A. Hrabar, A. Jentys, A. Lemonidou, J.A. Lercher, Journal of Catalysis 269 (2010) 411–420.
[15] A. Goguet, M. Aouine, F.J. Cadete Santos Aires, A. De Mallmann, D. Schweich, J.P. Candy, Journal of Catalysis 209 (2002) 135–144.
[16] N. Luo, X. Fu, F. Cao, T. Xiao, P.P. Edwards, Fuel 87 (2008) 3483–3489.
[17] F. Pompeo, D. Gazzoli, N.N. Nichio, Materials Letters 63 (2009) 477–479.
[18] L.W. Ho, C.P. Hwang, J.F. Lee, I. Wang, C.T. Yeh, Journal of Molecular Catalysis A: Chemical 136 (1998) 293–299.
[19] S. Jongpatiwut, N. Rattanapuchapong, T. Rirksomboon, S. Osuwan, D.E. Resasco, Catalysis Letters 122 (2008) 214–222.
[20] H. Lieske, G. Lietz, H. Spindler, J. Volter, Journal of Catalysis 81 (1983) 8–16.
[21] V.A. Mazzieri, J.M. Grau, J.C. Yori, C.R. Vera, C.L. Pieck, Applied Catalysis A: General 354 (2009) 161–168.
[22] M.J. Tiernan, O.E. Finlayson, Applied Catalysis B: Environmental 19 (1998) 23–35.
[23] L.F. Liotta, A. Longo, G. Pantaleo, G. Di Carlo, A. Martorana, S. Cimino, G. Russo, G. Deganello, Applied Catalysis B: Environmental 90 (2009) 470–477.
[24] K. Lehnert, P. Claus, Catalysis Communications 9 (2008) 2543–2546.
[25] H. Iida, A. Igarashi, Applied Catalysis A: General 298 (2006) 152–160.
[26] S. Ricote, G. Jacobs, M. Milling, Y. Ji, P. Patterson, B. Davis, Applied Catalysis A: General 303 (2006) 35–47.
[27] A.E. Nelson, K.H. Schulz, Applied Surface Science 210 (2003) 206–221.
[28] M.V. Rama Rao, T. Shripathi, Journal of Electron Spectroscopy and Related Phenomena 87 (1997) 121–126.
[29] J.Z. Shyu, K. Otto, W.L.H. Watkins, G.W. Graham, R.K. Belitz, H.S. Gandhi, Journal of Catalysis 114 (1988) 23–33.